Article **Journal of Technical Invention**
December 2022 Vol.6 No.18 11-17

Design and validation of a control for a BLDC motor to be applied on a solar water pump

Diseño y validación de un control para motor BLDC para aplicarse en una bomba solar de agua

HERRERA-VELÁZQUEZ, Rene[1]†, RODRIGUEZ-MEJIA, Jeovany Rafael*[2], LÓPEZ-MÁRTINEZ, Alfonso[1], and ARAIZA-ESQUIVEL, Ma. Auxiliadora[1]

[1]*Universidad Autónoma de Zacatecas, Unidad Académica de Ingeniería Eléctrica*
[2]*Departamento Metal-Mecánica Tecnológico Nacional de México Campus Ciudad Juárez*

ID 1st Author: *Rene, Herrera-Velázquez* / **ORC ID**: 0000-0003-2025-6882

ID 1st Co-author: *Jeovany Rafael, Rodriguez-Mejia* / **ORC ID**: 0000-0003-4154-0778

ID 2nd Co-author: *Alfonso, López-Mártinez* / **ORC ID**: 0000-0001-8547-9468

ID 3rd Co-author: *Ma. Auxiliadora, Araiza-Esquivel* / **ORC ID**: 0000-0001-8052-7483

DOI: 10.35429/JOTI.2022.18.6.11.17 Received July 12, 2022; Accepted December 24, 2022

Abstract

This paper presents the design and implementation of a speed control for BLDC motors; This is considered a high-capacity actuator mainly because of its operation, power, and control characteristics. BLDC motors require digital tools for good practices in position and speed control; as well as the power electronics for optimal performance. In order to take better advantage of the characteristics in this type of motor, a control strategy is presented that allows integrating the internet of things, to monitor and satisfy the needs when applied to a BLDC motor, which will also allow driving a submersible pump. Based on these characteristics, it will be possible to have a greater range of operation of the same, consequently, a better regulation of the speed, so that the desired water flow can be provided in the application of solar pumping systems. The results obtained validate the control designed for speed regulation in the system.

BLDC Motors, Control, Arduino, IGBT

Resumen

En este trabajo se presenta el diseño e implementación de un control de velocidad para motores BLDC; este es considerado como un actuador de alta capacidad principalmente por sus características de operación, alimentación y control. Los motores BLDC requieren de herramientas digitales para las buenas prácticas en el control de posición y velocidad; así como de la electrónica de potencia para su óptimo desempeño. Con el objetivo de aprovechar mejor las características en este tipo de motores se presenta una estrategia de control que permite integrar el internet de las cosas, para monitorear y satisfacer las necesidades al aplicarse en un motor BLDC, el cual además permitirá accionar una bomba sumergible. En base a estas características será posible tener un mayor rango de operación de la misma, en consecuencia, una mejor regulación de la velocidad, de forma que se pueda proporcionar el caudal de agua deseado en la aplicación de sistemas de bombeo solar. Los resultados obtenidos validan el control diseñado para la regulación de velocidad en el sistema.

Motores BLDC, Control, Arduino, IGBT

Citation: HERRERA-VELÁZQUEZ, Rene, RODRIGUEZ-MEJIA, Jeovany Rafael, LÓPEZ-MÁRTINEZ, Alfonso, and ARAIZA-ESQUIVEL, Ma. Auxiliadora. Design and validation of a control for a BLDC motor to be applied on a solar water pump. Journal of Technical Invention. 2022. 6-18: 11-17

*Correspondence to Author (e-mail: jrodriguez@itcj.edu.mx)
†Researcher contributing as first author.

I. Introduction

Electric motors are an integral part of industrial, residential and commercial plants, which mainly use conventional technologies to power them [1], [2]. Typically, the machines found in these appliances are single-phase induction motors or brushed direct current (DC) machines which are characterized by low efficiency and high maintenance requirements.

Brushless Direct Current (BLDC) brushless DC motors have reached a level of utility of great importance in industrial applications (robotics, aviation and automation) [3], they do not use brushes to energize the coils. Instead, they switch is done electronically; avoiding losses due to friction and wear. Furthermore, the torque and size ratio is much higher, making them useful in work environments with reduced space.

Induction motors have limitations in applications with little space. Moreover, they generate significant heat, which results in lower efficiency [2], [3]. Some of the advantages in BLDC motors compared to conventional DC motors are [4]: better speed-torque ratio, better dynamic response, higher efficiency and useful life, lower noise, higher speed range. Resulting in better performance than DC and induction motors, this type of motor is rapidly gaining popularity.

The main disadvantage of BLDC motors is their higher cost and a relatively higher degree of complexity of the power electronic converter used to power the motor [5]. For most applications, proportional-integral (PI) speed and current compensators are sufficient to establish an acceptable speed/torque controller. In other cases, state feedback control is needed to achieve more precise control of the BLDC motor [6]. Hysteresis current control and pulse width modulation (PWM) together with continuous control theory have generated the most widely used BLDC motor control techniques [7]. Complementarily, the discrete control theory allows such controllers to be implemented digitally with microcontrollers, microprocessors or digital signal processors (DSP) [6].

The objective of the proposed control strategy is that the BLDC motor achieves a regulation speed such that the drive pump provides the desired flow rate.

This work is organized as follows. Section 2 presents the structure and operation of the BLDC engine. Section 3 shows the mathematical model of the BLDC motor to design a controller. Sections 4 contains the results of a controller designed and implemented. Finally, section 5 shows the conclusions.

II. Structure and operation of the BLDC motor

BLDC motors are synchronous type motors whose magnetic fields exist in the stator and in the rotor rotate at the same frequency. Out of the different configurations, the triphasic is mostly used [8]. Fig. 1 shows the characteristic waveforms for a three-phase BLDC motor with trapezoidal flux distribution. A three-phase bridge with MOSFETs is necessary to energize the coils so that they commute as shown in Fig 2.

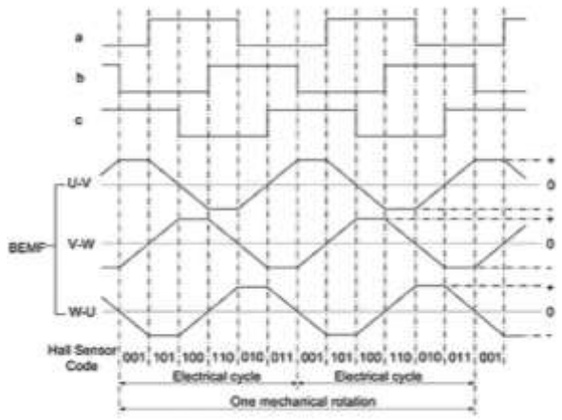

Figure 1 Hall Effect & Back EMF Signals
(https://www.digikey.com/es/articles/how-to-power-and-control-brushless-dc-motors)

The control technique used in the BLDC motor is the six step mode [9]. This strategy allows to control the current that circulates through the terminals of the motor coils, activating 2 coils at the same time and leaving the third one off [10]. The pair of on-coils are successively alternated until completing the six possible cases. as shown in Fig. 2. The output stage consists of a three-phase inverter composed of MOSFETs as shown in Fig. 3.

ISSN 2523-6792

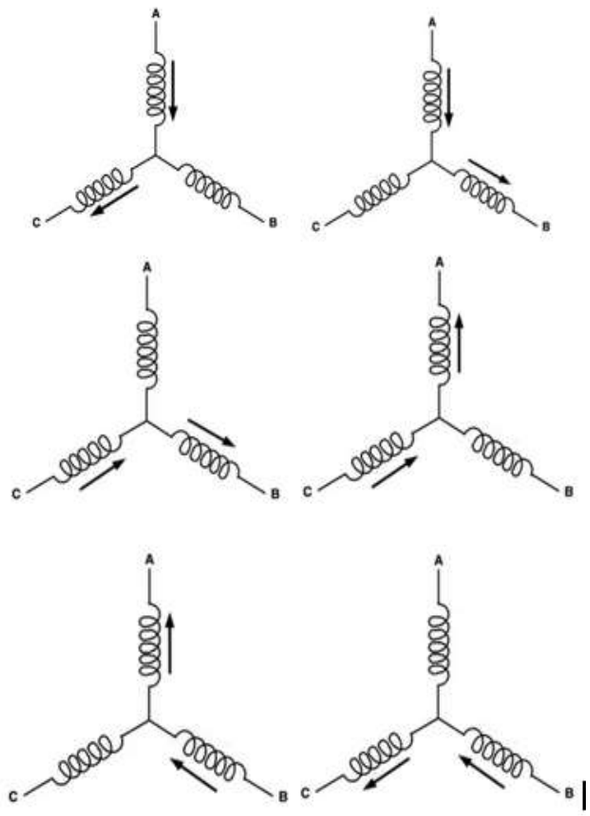

Figure 2 Coil commutation in three-phase bridge
(https://www.digikey.com.mx/es/articles/controlling-sensorless-bldc-motors-via-back-emf)

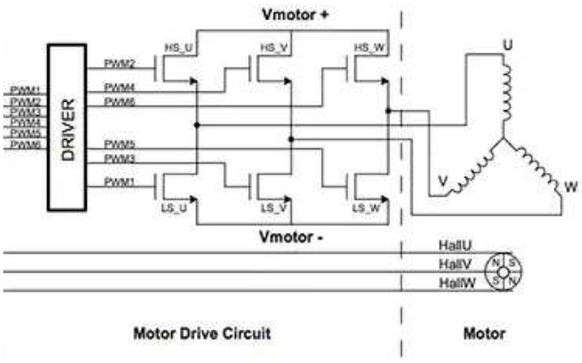

Figure 3 Three-phase bridge
(https://www.digikey.com/es/articles/how-to-power-and-control-brushless-dc-motors)

In the case of the BLDC motor, it contains a fixed part (stator), where the windings are located, and a moving part (rotor) of permanent magnets [11]. The BLDC motor requires an electronic circuit that acts as a commutator, which allows control of the position and direction of rotation, see Fig. 4.

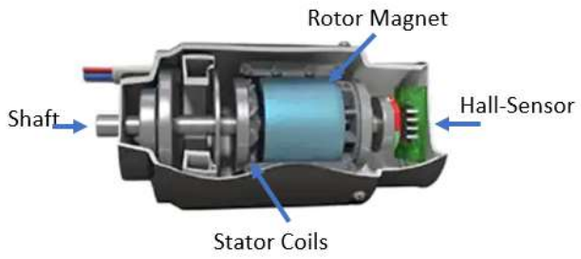

Figure 4 Motor BLDC diagram
(https://www.digikey.com/es/articles/how-to-power-and-control-brushless-dc-motor)

III. Mathematical model of the BLDC motor

The mathematical model of the BLDC motor does not differ much from that of a conventional DC motor, as represented by the three-phase configuration shown in Fig. 5.

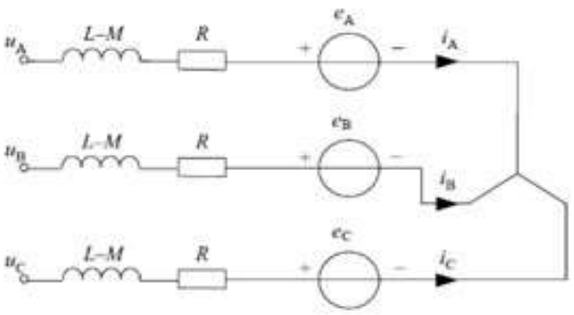

Figure 5 Equivalent circuit of a BLDC motor
Source: Own Elaboration

The equations that describe its electromechanical behavior are:

$$u_A = Ri_A + (L - M)\frac{di_A}{dt} + e_A \quad (1)$$

$$u_B = Ri_B + (L - M)\frac{di_B}{dt} + e_B \quad (2)$$

$$u_C = Ri_C + (L - M)\frac{di_C}{dt} + e_C \quad (3)$$

$$i_A + i_B + i_C = 0 \quad (4)$$

Where the voltage of the phases A, B, C are given by (1), (2) and (3), Since the windings are symmetric the resistance R, the inductance L and the mutual inductance M for these phases are the same. [12]. Likewise, the currents of the three phases i_A,i_B,i_C must fulfill the conditions of (4) . Applying Kirchhoff's voltage law to the circuit, the line voltages u_{AB}, u_{BC}, u_{CA} are obtained.

$$u_{AB} = R(i_A - i_B) + (L - M)\frac{di_A}{dt} + (M - L)\frac{di_B}{dt} + (e_A - e_B) \quad (5)$$

$$u_{BC} = R(i_B - i_C) + (L - M)\frac{di_B}{dt} + (M - L)\frac{di_C}{dt} + (e_B - e_C) \quad (6)$$

$$u_{CA} = R(i_C - i_A) + (L - M)\frac{di_C}{dt} + (M - L)\frac{di_A}{dt} + (e_C - e_A) \quad (7)$$

where the counter-electromotive forces (EMF) induced in the stator windings and the electric torque are expressed as:

$$e_A = \frac{K_e}{2}F(\theta) \quad (8)$$

$$e_B = \frac{K_e}{2}F(\theta - \frac{2\pi}{3}) \quad (9)$$

$$e_C = \frac{K_e}{2}F(\theta - \frac{4\pi}{3}) \quad (10)$$

$$T_e = \frac{K_e}{2}(F(\theta)i_A + (F\left(\theta - \frac{2\pi}{3}\right)i_B + F\left(\theta - \frac{4\pi}{3}\right)i_C \quad (11)$$

where K_e is the constant for the counter electromotive force [12], [13]. The counter electromotive force presents a trapezoidal waveform along the electric angle θ, and is defined by the function F(θ) that is bounded in the interval [-1,1]. A period of this function is defined as:

$$F(\theta)\begin{cases} 1 & 0 \le \theta < \frac{2\pi}{3} \\ 1 - \frac{6}{\pi}\left(\theta - \frac{2\pi}{3}\right) & \frac{2\pi}{3} \le \theta < \pi \\ -1 & \pi \le \theta < \frac{5\pi}{3} \\ -1 + \frac{6}{\pi}\left(\theta - \frac{5\pi}{3}\right) & \frac{5\pi}{3} \le \theta < 2\pi \end{cases} \quad (12)$$

where the electric angle θ of the electric field induced in the stator is directly related to the mechanical angle θ_m which is determined on the circumference of the motor. Thus, we have:

$$\theta = \theta_m \frac{p}{2} \quad (13)$$

where ρ is the number of poles. Therefore, the speed of the rotor and its position is related as:

$$\frac{d\theta}{dt} = \frac{p}{2}w_m \quad (14)$$

If the electric torque is defined as:

$$T_e = \frac{i_A e_A + i_B e_B + i_C e_C}{w_m} \quad (15)$$

then the electromagnetic power is equivalent to the power transferred to the rotor, being equal to the ratio between the electrical torque and the mechanical speed.

$$P_e = T_e w_m \quad (16)$$

Finally, there is the mechanical subsystem, which does not vary with respect to that of the conventional DC motor [14].

$$T_e = K_f w_m + J\frac{dw_m}{dt} + T_L \quad (17)$$

IV. Results

Using the Proteus application, the construction of the control circuit was carried out, in this application the scheme was designed: the electronics, software programming, simulation set-up, debugging, documentation and construction (Proteus has a library that allows the mounting of the programming code on the Arduino virtual board in Proteus). In the Fig. 6 electronic part (hardware) IR2101 are the drivers used to amplify the applied voltage in the gates of the MOSFETs.

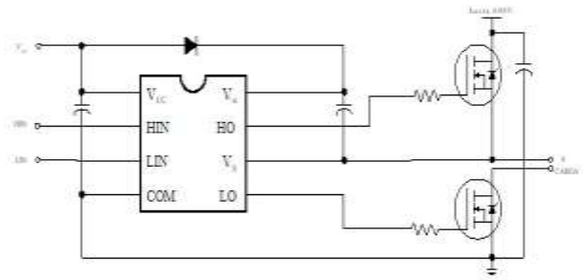

Figure 6 Typical connection for IR2101 driver (*Data Sheet No. PD60043 Rev.O www.irf.com)*

Fig. 7 shows the circuit design and the assembly of the same.

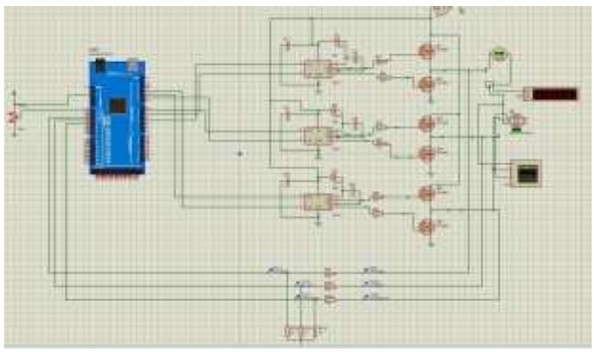

Figure 7 Simulation of the circuit in proteus
Source: Own Elaboration

Once the circuit is ready, the code is loaded into the Virtual Arduino. Next, the simulations were performed and the signals were obtained as shown in Fig. 8.

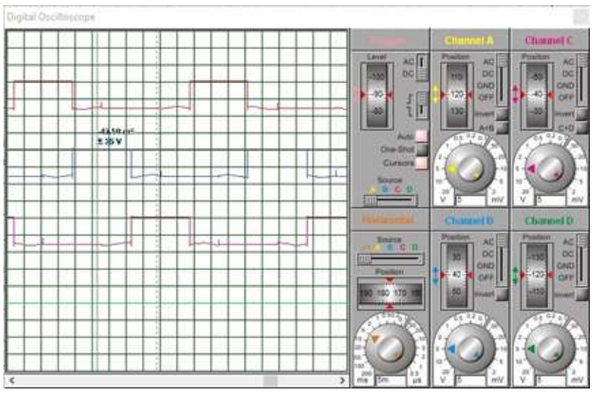

Figure 8 Simulated pulses in proteus
Source: Own Elaboration

The simulations allowed the verification of the Programming code operation. As shown in figure 9, the circuit was printed. It was programmed in PCB programming. The assembled components were three IR2101 drivers and six MOSFETs.

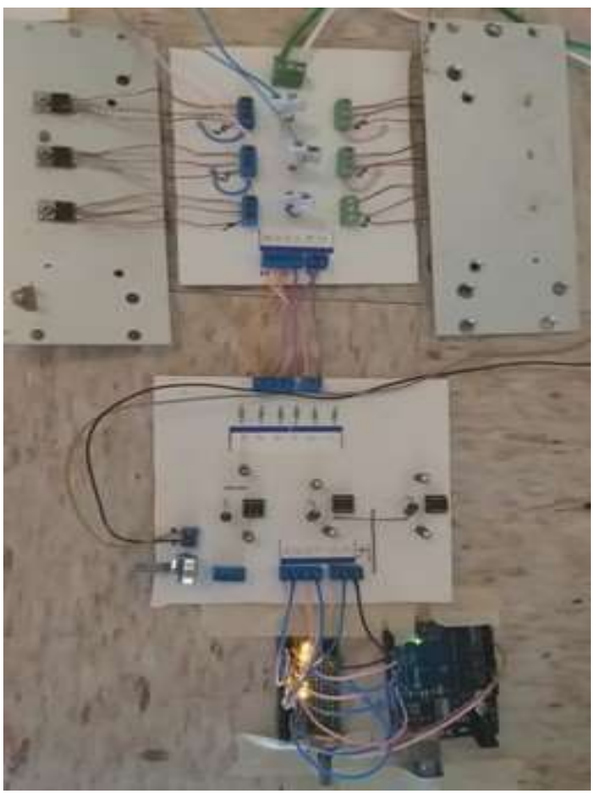

Figure 9 Circuit implemented with IR2101 drivers
Source: Own Elaboration

Fig. 10 shows the outputs of the implemented system, It can be seen that the signals obtained approximate.

Those obtained in the simulation; allowing the verification of the control expectations and the correspondence of the prototype signals with the simulation signals.

Figure 10 Output signals of the IR2101 drivers
Source: Own Elaboration

The results in Table 1 show the efficacy of the Controller. Observing that, by varying the frequency the engine speed increases and decreases; noting that the system adjusts to the frequency change and stabilizes the RPM smoothly. It also maintains its speed until it is necessary to vary again. Correspondence is found by observing the phase time of the signals arriving to the engine; since the output of the system and the simulation these signals are similar.

Velocity (RPM)	Freq. (Hz)	Time of Fase (µs)
518	57.48	29.97
735	69	24.44
833	81.5	21
910	92.34	17.96
1008	103.9	16.24
1106	125.1	13.38
1197	148.8	12.24
1350	166.4	11.67
1393	171.5	10.9
1463	197.1	9.57
1624	205.5	9.13
1729	222.5	8.19

Table 1 Data of obtained parameters of controller BLDC
Source: Own Elaboration

Table 2 shows the engine's RPM, these are defined as value read with the encoder sensor (RPMM), and value obtained in simulation or expected value (RPMS) respectively. The root mean square error (RMSE) presents the difference between these two values, between the set of RPMM and RPMS data. The standard deviation and the Pearson's correlation coefficient are also shown. It is also noted an index of low dispersion, maintaining the parameters statistics within standard ranges.

ISSN 2523-6792

Dispersion Statistics	RPM_O	RPM_S	$RPM_S - RPM_O$
	518	535	-17
	735	663	72
	833	788	45
	910	874	36
	1008	992	16
	1106	1194	-88
	1197	1289	-92
	1350	1394	-44
	1393	1432	-39
	1463	1585	-122
	1624	1652	-28
	1729	1719	10
Standard deviation	370.58	400.51	
RMSE			66.70
Pearson's´Coefficient			0.991

Table 2 RPM, RMSE and SDV
Source: Own Elaboration

Fig. 11 graphically shows the behavior of the motor at different values of frequency, which demonstrates that the controller complies with the regulatory expectations of engine speed.

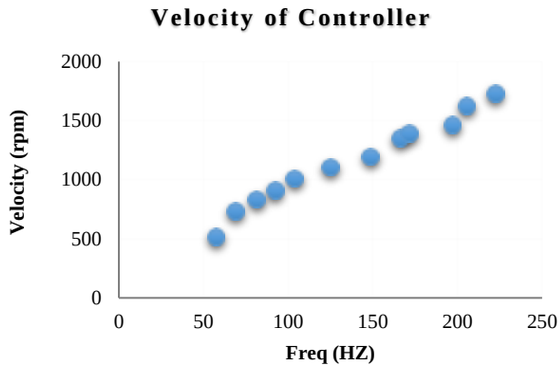

Figure 11 RPM vs Frequency curve
Source: Own Elaboration

V. Conclusion

In this work it was possible to verify that the control proposal made for the BLDC motor was satisfactory since a better range of speed variation was achieved both in the simulated design and in the built system. In addition, the system did not present RPM stability problems when intentionally varying the frequency.

In conclusion, due to the characteristics of the BLDC motor that submersible water pumps have, the simplicity and low cost of the controller that was designed, simulated, built and validated make it attractive for use in application systems. of solar pumping in the regions of Zacatecas.

In addition, it is noteworthy to say that the design of the controller can be integrated into systems with monitoring and industry 4.0 applications where the use of the Internet of Things makes it more efficient and adds value to solar pumping irrigation systems. Therefore, the use of platforms such as Arduino allows us to expand the capabilities of a control system in such a way that using a complement that includes internet (WiFi) it can be monitored or reprogrammed through the use of the internet of things and the new trend of I 4.0.

One of the authors (R.H.V.) thanks CONACYT for the partial support for carrying out this work with CVU: 896183. Prototype: This work has been funded by CONACYT [grant number 896183, 2018].

VI. References

[1] R. Kandiban and R. Arulmozhiyal, (2012), "Design of Adaptive Fuzzy PID Controller for Speed control of BLDC Motor," *Int. J. Soft Comput. Eng.*, vol. 2, no. 1, pp. 386–391, 2012. https://www.ijsce.org/wp-content/uploads/papers/v2i1/A0458022112.pdf

[2] F. Aghili, (2011), "Fault-tolerant torque control of BLDC motors," *IEEE Trans. Power Electron.*, vol. 26, no. 2, pp. 355–363, 2011. https://ieeexplore.ieee.org/document/5535190

[3] C. T. Lin, C. W. Hung, and C. W. Liu, (2008), "Position sensorless control for four-switch three-phase brushless DC motor drives," *IEEE Trans. Power Electron.*, vol. 23, no. 1, pp. 438–444, 2008. http://ntur.lib.ntu.edu.tw/bitstream/246246/151885/1/75.pdf

[4] Padmaraja Yedamale, (2003), "AN885 Brushless DC (BLDC) Motor Fundamentals", Microchip Technology Inc. 2003 http://ww1.microchip.com/downloads/en/AppNotes/00885a.pdf

[5] S. A. R. Sierra, (2013), "Control híbrido de motores DC sin escobillas usando FPGA,Tesis," INAOE, 2013. https://inaoe.repositorioinstitucional.mx/jspui/bitstream/1009/241/1/ReyesSSA.pdf

[6] M. R. ARNAL, (2002), “Estimación de posición y control simplificado de corriente para motores BLDC, usando tecnología DSP” , Tesis, Universidad Catolica De Chile Escuela De Ingenieria, 2002. https://www.researchgate.net/publication/34752607_Estimacion_de_posicion_y_control_simplificado_de_corriente_para_motores_BLDC_usando_tecnologia_DSP

[7] C. S. Joice, S. R. Paranjothi, and V. J. S. Kumar, (2017), “Digital control strategy for four quadrant operation of three phase BLDC motor with load variations,” *Int. J. Innov. Technol.*, vol. 9, no. 2, pp. 0028–0032, 2017. https://ieeexplore.ieee.org/document/6319386

[8] Seminario Gastelo J. M., (2021), “Diseño de controlador de velocidad de motor brushless DC mediante la fuerza contraelectromotriz,”,Tesis, Universidad De Piura, 2021. https://pirhua.udep.edu.pe/bitstream/handle/11042/5357/IME_2119.pdf?sequence=1&isAllowed=y

[9] B. Alecsa and A. Onea, (2010), "Design, validation and FPGA implementation of a brushless DC motor speed controller," Electronics, Circuits, and Systems (ICECS), 2010 17th IEEE International Conference on Athens, Greece, pp. 1112-1115, 2010. https://ieeexplore.ieee.org/document/5724711

[10] C.-T. Lin, C.-W. Hung, and C.-W. Liu, (2006), "Sensorless Control for Four-Switch Three-Phase Brushless DC Motor Drives," Industry Applications Conference, 2006. 41st IAS Annual Meeting. Conference Record of the 2006 IEEE , pp. 2048-2053, 2006. https://ieeexplore.ieee.org/document/4025505

[11] R. Arulmozhiyal and R. Kandiban, (2012), "Design of Fuzzy PID controller for Brushless DC motor," Computer Communication and Informatics (ICCCI), 2012 International Conference on Coimbatore, India, pp. 1-7, 2012. https://ieeexplore.ieee.org/document/6158919

[12] M.-F. Tsai, T. P. Quy, B.-F. Wu, and C.-S. Tseng, (2011), "Model construction and verification of a BLDC motor using MATLAB/SIMULINK and FPGA control," Industrial Electronics and Applications (ICIEA), 2011 6th IEEE Conference on Beijing, China, pp. 1797-1802, Jun. 2011. https://ieeexplore.ieee.org/document/5975884

[13] B. Alecsa and A. Onea, (2010), "An FPGA implementation of a brushless DC motor speed controller," Design and Technology in Electronic Packaging (SIITME), 2010 IEEE 16th International Symposium for Pitesti, Romania, pp. 99-102, 2010. https://ieeexplore.ieee.org/document/5653617

[14] Castillo Amaya, J. D. (2022). Desarrollo de actuadores altamente dinámicos con aplicaciones en robótica bio-inspirada. https://repositorio.uvg.edu.gt/handle/123456789/4269

ISSN 2523-6792